J. Fluid Mech. (1984), *vol.* 147, *pp.* 449–464
Printed in Great Britain

Nonlinear forces on a horizontal cylinder beneath waves

By JOHN R. CHAPLIN
Department of Civil Engineering, University of Liverpool

(Received 2 March 1984 and in revised form 31 May 1984)

Measurements of forces experienced by a submerged horizontal cylinder with its axis parallel to the crests in deep-water waves reveal nonlinear components with frequencies up to three times the fundamental wave frequency. The dominant nonlinear contribution to the loading is at the third order in the wave amplitude, and, for Keulegan–Carpenter numbers approaching 2, its magnitude was found to be as much as one-half that of the inertia force. It is suggested that the third-order force is associated with circulation generated by steady streaming in the oscillatory boundary layer on the cylinder. At higher Keulegan–Carpenter numbers, form drag becomes increasingly important, and velocity measurements close to the cylinder show the rapid development of the wake. Observations of nonlinear features of the transmitted waves are also discussed.

1. Introduction

It is well known that, according to linear theory, surface waves in deep water suffer a phase shift in passing over a submerged cylinder with its axis parallel to the crests. This was first proved by Dean (1948), who showed also that to the same approximation there are no waves reflected from the cylinder. Ogilvie (1963) later applied Ursell's (1950) procedure to derive, from the first-order velocity potential, expressions for the forces on the cylinder arising from it. More recently, alternative and more general solutions to the linearized irrotational-flow problem of the effects of the cylinder on the waves have been given by Leppington & Siew (1980), Mehlum (1980) and Grue & Palm (1984). For the case of the circular cylinder, their conclusions are identical with Dean's, and, in developing the velocity potential only to first order, they are unable to make any advance in calculating the nonlinear forces beyond those derived by Ogilvie. A numerical solution to the nonlinear problem by Stansby & Slaouti (1984) for waves of more than 50% limiting height yielded for the fluctuating force values which agree with Ogilvie's theory to within 3% for Keulegan–Carpenter numbers up to 1.2. This suggests that the errors arising from the assumptions of the linearized analyses of the inviscid flow in this range are not severe.

However, in addition to the nonlinearities of the inviscid flow, there remain those that arise from the action of viscosity. In related contexts (Longuet-Higgins 1970; Riley 1971, 1978), the external irrotational flow is modified by the effects of steady streaming which is generated in the oscillatory boundary layer at the cylinder's surface. In the present circumstances a consequence of streaming flow is a steady circulation around the cylinder, and from measurements of the induced steady flow and of the fluctuating pressures at the cylinder's surface Chaplin (1984) suggested that the circulation gives rise to a significant nonlinear lift in antiphase with the inertia force.

It is the purpose of this paper to study nonlinear features of the loading on the cylinder and its effects on the waves, by means of the analysis of experimental measurements made in conditions in which the Keulegan–Carpenter number is less than 3. The implications of theoretical analyses for the inviscid and viscous flows are reviewed in §§2 and 3. Following a description of the experimental method in §4, §5 presents force and velocity measurements, and shows that in the fluctuating force there is a strong third-order component which renders Ogilvie's solution rather inaccurate for waves of moderate steepness, before form drag becomes significant. Nonlinear features of the transmitted waves are described in §6.

2. The inviscid flow

From the first-order velocity potential for the flow around a horizontal cylinder submerged beneath waves in deep water, Ogilvie (1963) derived expressions for the first-order force on the cylinder (i.e. the force component that is proportional to the wave amplitude a when other independent parameters remain constant) and the time-independent part of the second-order force (proportional to a^2). The horizontal and vertical components of the first-order force have equal magnitudes, and oscillate in quadrature with the wave period $2\pi/\omega$. Besides the time-independent part of the second-order force, which acts vertically upwards, there is a second-order unsteady force with frequency 2ω. Furthermore, Ogilvie showed that the first-order force on the cylinder lags the local acceleration in the undisturbed flow at the cylinder's axis by a phase angle which is one-half that suffered by the waves in passing over the cylinder. It is clear from the nonlinearity of the free-surface boundary condition that, unless the cylinder is deeply submerged, there are also higher-order forces whose frequencies are the sums and differences of those at lower orders. Without a solution for the nonlinear velocity potential, however, it is not clear at what frequencies the higher-order forces will appear. The inviscid flow around a cylinder that is submerged at sufficient depth for its effect at the free surface to be neglected can be analysed by means of Milne-Thomson's circle theorem. Proceeding on this basis, Chaplin (1981) showed that in the limiting case the force on the cylinder consists *only* of the first-order force at frequency ω and the second-order steady force, and that this is a good approximation to Ogilvie's solution provided that the submergence $-y_0/c$ exceeds about 5 (see figure 1).

In reality, whether the cylinder is deeply submerged or not, increasing the wave amplitude may ultimately cause the flow around it to be dramatically changed by the occurrence of separation, and the force to be dominated by form drag. It is a purpose of this paper to determine experimentally whether, before this takes place, significant nonlinear forces can arise, either from other effects of viscosity or from the free-surface nonlinearity.

In order to present forces in dimensionless terms, we express the magnitudes of the x- and y-components of the force per unit length of cylinder at frequency $n\omega$ as

$$F_x^{(n)} = \sum_m C_{xnm}\rho c^3\omega^2 K_c^m; \quad F_y^{(n)} = \sum_m C_{ynm}\rho c^3\omega^2 K_c^m, \tag{2.1}$$

where ρ is the fluid density. K_c is the Keulegan–Carpenter number, which for small-amplitude deep-water waves of wavelength $2\pi/k$ is given by

$$K_c = \frac{\pi a}{c} e^{ky_0}. \tag{2.2}$$

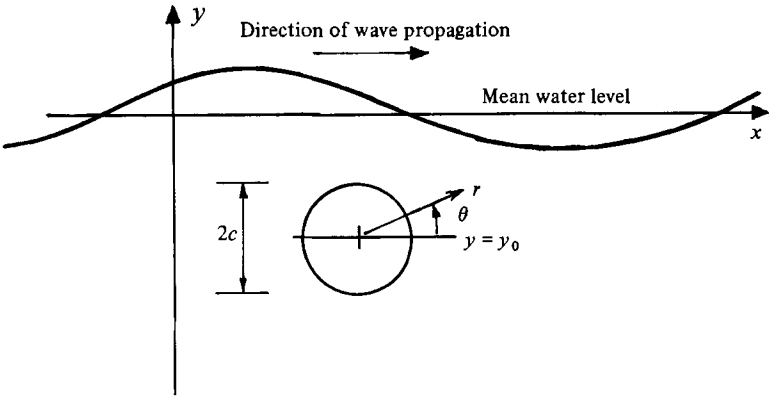

FIGURE 1. Definition sketch.

The dimensionless coefficients C are functions of kc and ky_0; from Ogilvie (1963, equations (27) and (28)) may be derived expressions for $C_{x11} = C_{y11}$ (the conventional inertia coefficient C_m which takes a limiting value of 2 when $-y_0 \gg c$ and $kc \ll 1$), C_{x02} (zero) and C_{y02}.

3. The viscous flow

The oscillatory boundary layer on the surface of the cylinder is of a mainly progressive nature, since the pattern of the external velocity distribution advances once around the cylinder in every wave period. Owing to the non-uniformity of the wave-induced external flow, the magnitude of the velocity fluctuation is a function of the angular position θ. But, unless the cylinder is located close to the free surface, or kc is large, it is reasonable to expect that the essential characteristics of the boundary layer are the same as those for a cylinder in uniform circular orbital flow (kinematically identical with the case of a cylinder progressing without rotation around a circular path in fluid initially at rest). In both uniform and non-uniform cases, steady streaming is generated within the boundary layer, so that there exists, at its outer edge, circulation around the cylinder with the same sense of rotation as that of the ambient orbital motion. Longuet-Higgins (1970) studied the uniform case in a rather different context, and showed that the steady streaming merges into the external irrotational flow in the form of a potential vortex around the cylinder with circulation

$$\Gamma = \frac{6\pi U_0^2}{\omega}, \tag{3.1}$$

where U_0 is the speed of the undisturbed flow.

The existence of such a vortex (with a strength independent of the viscosity) centred on the cylinder would, in the present context, have implications for the loading which the cylinder experiences. Measurements of the steady current just outside the boundary layer around a horizontal cylinder beneath waves were made by Chaplin (1984), who showed them to be in agreement with the predictions of Batchelor's (1967, equation (5.13.20)) general formula for steady streaming. In the limiting case of a small cylinder deeply submerged this reduces to (3.1). Modifications to the pressure distribution on the cylinder due to interaction between the circulation and the incident flow may be expected therefore to be proportional to U_0^3. However, even excluding the effects of separation, this is not the only contribution to the

pressure arising from the action of viscosity; for an analysis of the nonlinear boundary-layer problem we turn to the work of Riley (1971, 1978).

Riley (1971) analysed the uniform-flow case and derived the initial terms of perturbation solutions for the stream functions of the flow inside and outside the boundary layer. The solutions are formulated as double series with $M^{-1} = (\nu/\omega c^2)^{\frac{1}{2}}$ and $\epsilon = K_c/\pi$ as expansion parameters (Riley 1971 equation (19)); ν is the kinematic viscosity. By evaluating the tangential pressure gradient and the shear stress at the cylinder's surface from the dimensionless terms that Riley obtained from the inner expansion, namely the leading constant (linear) term, and terms in M^{-1} and ϵ, we obtain the following components of loading per unit length:

(i) the inertia force of magnitude $F_i = C_m \pi c^2 \rho U_0 \omega$, with the inertia coefficient $C_m = 2$, rotating at frequency ω in phase with the acceleration vector of the undisturbed flow;

(ii) a force of magnitude $F_i(2K_C/\pi R_e)^{\frac{1}{2}}$ resulting from normal stresses, rotating at frequency ω with a phase lag of $\frac{1}{4}\pi$ with respect to (i);

(iii) a force of magnitude $F_i(2K_C/\pi R_e)^{\frac{1}{2}}$ resulting from shear stresses, rotating at frequency ω with a phase lag of $\frac{1}{4}\pi$ with respect to (i);

(iv) a steady torque of $2F_i c(K_C^3/\pi^3 R_3)^{\frac{1}{2}}$; where $R_e = 2U_0 c/\nu$ is the Reynolds number.

The significance of forces (ii) and (iii) to the present experimental results is discussed in §5.

The uniform steady circulation (3.1) appears in Riley's (1971) outer expansion, and a corresponding steady term in the inner expansion (Riley 1971, equations (28) and (24) respectively). However, the circulation in the irrotational flow does not influence any of the force components given above, since the component of pressure to which it gives rise is proportional to U_0^3; the terms obtained in Riley's expansions do not extend to this order.

Considering only the inviscid flow, the circulation (3.1) would give rise to a lift of magnitude

$$F_l = 3F_i K_C^2/\pi^2, \tag{3.2}$$

in antiphase with the inertia force. Other (unknown) terms in the perturbation expansions will also contribute to the force at this order, through modifications to both viscous and inviscid flows. Therefore the main significance of (3.2) is that it represents a force which is independent of viscosity, and is of a magnitude comparable to that of the inertia force, for $K_C \sim 1$.

When the external flow is non-uniform (as in the present case), Riley (1978) showed that there exists an outer boundary layer which achieves the transition between the tangential velocity distributions of the streaming flow and the outer potential vortex. Numerical solutions for two particular cases showed that the steady circulation may then exceed that given by (3.1).

Ignoring the effects of separation, we may conclude that there is a component of force on the cylinder at frequency ω with third-order contributions (independent of Reynolds number, assuming laminar flow) both from the free-surface boundary conditions, and from the effects of steady streaming. In experimental results presented in §5, measurements of velocity close to the cylinder provide evidence of the occurrence of separation, and nonlinear force components are identified at frequencies 0, ω, 2ω and 3ω.

4. Experimental arrangement

The experiments were carried out in the 35 m long random-wave flume of the Department of Civil Engineering of Liverpool University. This flume is 600 mm wide and is equipped with an electromagnetically operated servo-controlled paddle system incorporating force feedback from the paddle face to minimize wave reflections. The mean water depth was 800 mm or 850 mm. The cylinder was mounted in the flume at a section 12 m from the paddle and 18 m from the toe of the beach. Experiments were controlled directly from a minicomputer, which generated the paddle command signal, carried out data acquisition and analysis, and waited a specified time between executing successive runs. In this way the timing of the experiments could be very closely controlled; all results given below for each case were computed from a sequence of eight waves beginning after at least the eighth wave in the train had passed the cylinder; data acquisition was completed before reflections from the beach had arrived at the working section, and there was sufficient delay between runs to ensure that the entire water surface became absolutely stationary. All channels were automatically zeroed immediately before each test, and were sampled simultaneously at 100 Hz with a 12-bit analog-to-digital converter.

For the purposes of measuring wave amplitudes and phases, four surface-elevation gauges were available at various intervals along the flume on the beach side of the cylinder, and three more on the paddle side. The total length of the wave-gauge array was 10.8 m.

Details of the cylinder are shown in figure 2. It consisted of a perspex tube of 102 mm outside diameter and length 546 mm, mounted between circular endplates of the same diameter, bringing the total length to approximately 600 mm. Stiff aluminium bars inside the cylinder ran between the endplates, one of which was equipped with an extension piece mounted on the threads of three thumbwheels. The cylinder could be fixed in any horizontal position spanning the flume by extending its length until it was jammed tightly between the flume's vertical walls. The perspex cylinder was mounted on two strain-gauged cantilevers built into the endplates. In order to seal the cylinder, the inside of which was dry throughout the experiments, the gaps between the perspex cylinder and the endplates were covered externally by thin latex sleeves, bonded with silicone rubber. Mounted in this way, the cylinder presented to the flow a profile uniform across the flume, interrupted only by the strain-gauge cables of about 3 mm diameter, which emerged vertically from the endplates and were taped to the flume walls. The strain gauges provided signals that were of high stability and very low noise, and from which the total horizontal and vertical force components on the cylinder were computed. The natural frequency of the cylinder in water was 22 Hz.

The cylinder was calibrated *in situ* by hanging masses of up to 1.2 kg from it, using a light pulley for the horizontal direction. Since some of the forces to be isolated from the measurements were rather small, the resolution of the strain-gauge system was also investigated, statically and dynamically. For the static test, the calibration was repeated using much smaller load increments. Applying the loads in 5 steps of 1 g produced a calibration within 10% of the original value, with a least-squares correlation coefficient greater than 0.985. In order to obtain the response of the cylinder to small oscillating loads, a mass was hung from its central section on a thread 1 m long. By swinging the mass with a measured displacement in the plane perpendicular to the cylinder's axis, known horizontal and vertical oscillatory loads of periods 2 s and 1 s respectively were applied to the cylinder. At amplitudes of 0.05

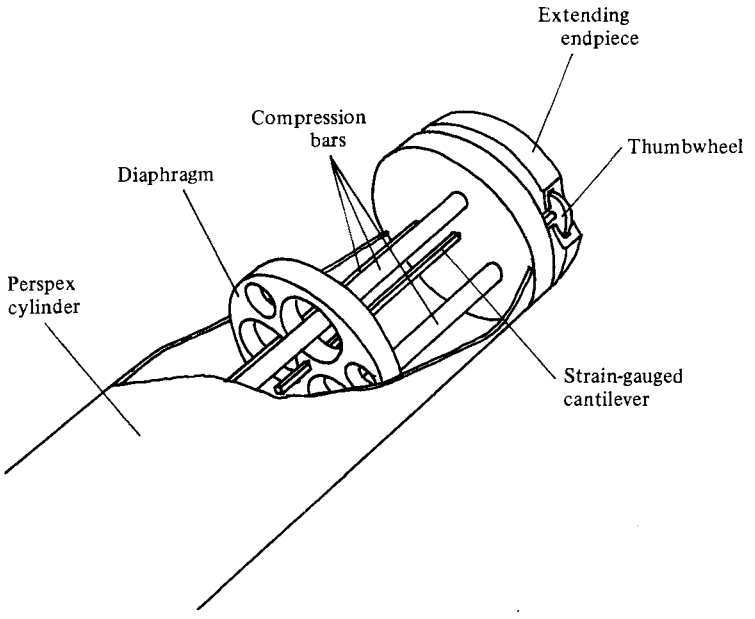

FIGURE 2. Construction of test cylinder.

and 0.02 N the measured forces were found to be in error by less than 6% and 13% respectively. With a measurement system of this quality, it was felt that reliable force data could be obtained at least down to amplitudes of 0.05 N. In most cases the measured magnitudes of the force components that form the subject of this work were considerably in excess of 0.5 N.

Velocity measurements were made with a 2-channel DISA laser anemometer operating in forward scatter with polarization separation. In all tests the measurement volume was positioned at the elevation of the cylinder's axis, and in most cases at a distance of several diameters from it, in order to provide a check on the incident flow velocity independent of the wave-gauge records. However, in some tests the tangential velocity much closer to the cylinder was measured for the purpose of identifying its wake.

5. Force and velocity measurements

The conditions for which measurements were made are set out in table 1. In all cases except A the waves were nominally in deep water, having $kd > \pi$. The tests of case A were undertaken in order to achieve Keulegan–Carpenter numbers large enough to give clear evidence of a wake when the cylinder was at a submergence sufficient for its influence on the free surface to be unimportant. For case A the ratio of vertical to horizontal particle velocity amplitudes in the undisturbed flow at the cylinder's elevation was about 0.92.

Typical records of the clockwise velocity component at the location $r/c = 1.04, \theta = 0$ (see figure 1) are shown in figure 3(*a*). At $K_c = 1.08$ (based on the horizontal flow component) the velocity trace follows a smooth oscillation interrupted only by small intermittent irregularities at the instants when the clockwise tangential velocity has a maximum. In larger waves these disturbances become relatively stronger; at $K_C = 1.47$ there are significant irregular reductions in velocity at the measurement

Case	Period (s)	Water depth (mm)	$\frac{y_0}{c}$	kc	kd	$\frac{R_e}{K_C}$
A	1.2	800	−5	0.146	2.28	7600
B	1.0	850	−5	0.206	3.43	9120
C	1.0	850	−3	0.206	3.43	9120
D	0.75	850	−2	0.365	6.08	12200
E	1.0	850	−2	0.206	3.43	9120
F	0.75	850	−2	0.365	6.08	12200
G	0.6	850	−2	0.570	9.50	15200
H	0.5	850	−2	0.821	13.7	18300

TABLE 1. Experimental conditions

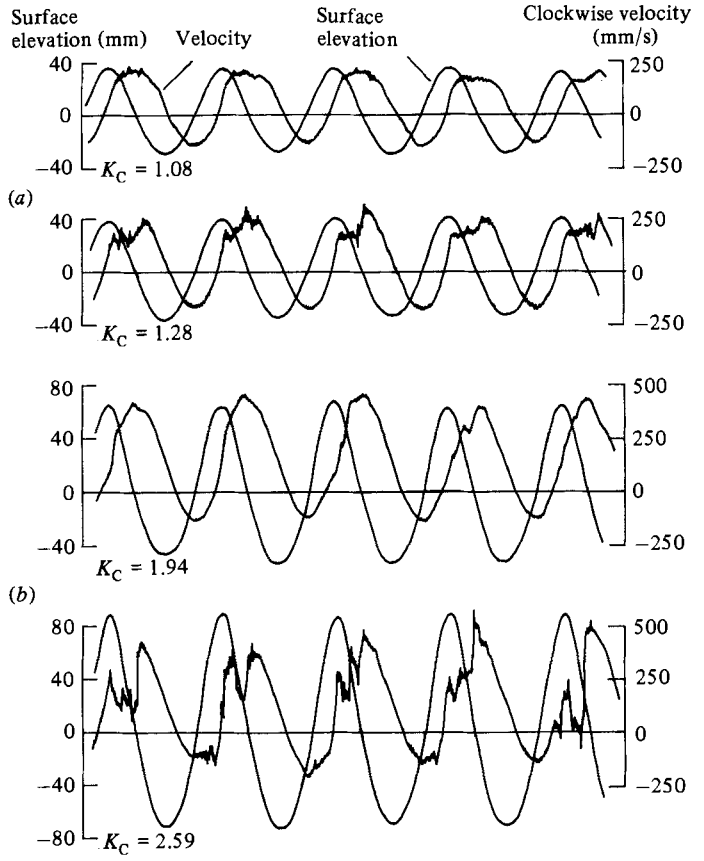

FIGURE 3. Records of the clockwise tangential velocity component, case A: (*a*) at $r/c = 1.04$, $\theta = 0°$; (*b*) at $r/c = 1.28$, $\theta = 0°$. The positive mean value of the velocity records is the effect of clockwise circulation.

point as the wake of the cylinder is swept past, contrasting with the smooth flow at other times. The lowest Keulegan–Carpenter number at which this was observed was found to be a function of the distance of the measurement point from the cylinder. At $r/c = 1.04$, 1.07, 1.28 smooth velocity records were obtained up to approximately $K_C = 1.1$, 1.5 and 2.2 respectively. For K_C less than about 2, these results suggest that the wake is closed, that its size increases with K_C, and that it progresses around

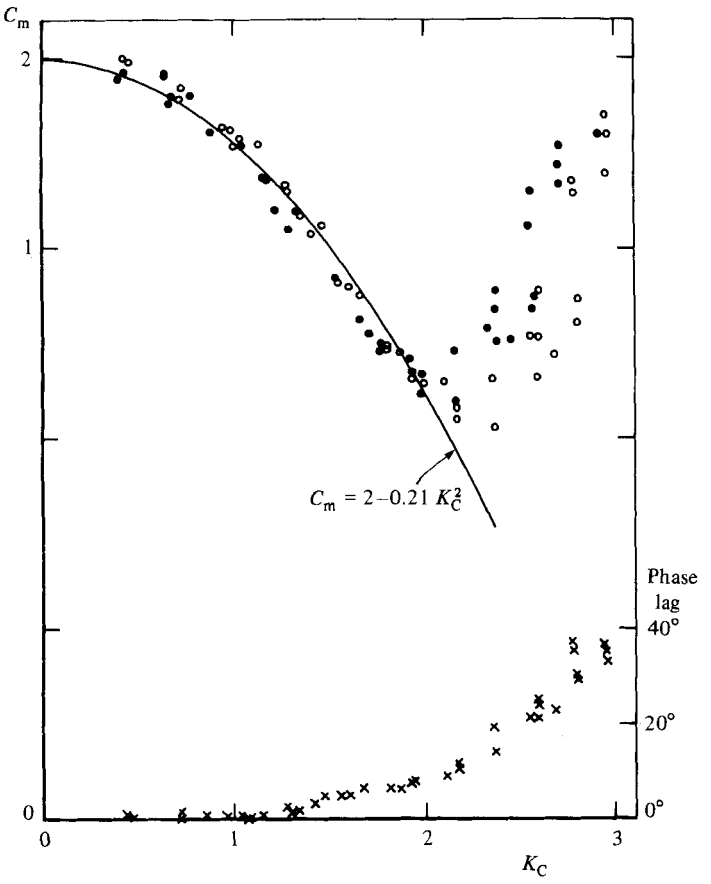

FIGURE 4. Inertia coefficient, case A: ●, horizontal force; ○, vertical force. Phase lag of the force at the wave frequency with respect to the acceleration of the incident flow: ×.

the cylinder at the wave frequency. For larger values of K_C, however, the irregularities in the velocity traces become much more dramatic (as shown in figure 3*b*), and at $K_C = 2.6$ they were detected in velocity measurements as far from the cylinder as $r/c = 6.4$. It is concluded that, although separation occurs at lower Keulegan–Carpenter numbers, there is a critical value in the region of 2 where the wake first breaks away from the cylinder, generating large-scale disruption in the irrotational flow.

Force measurements at the wave frequency from case A are presented in figure 4 in terms of the inertia coefficient C_m plotted against K_C. With increasing K_C there is a progressive reduction in C_m from the value of 2, following a parabolic relationship as shown. At $K_C \approx 2$ there is a sudden departure from this trend and a marked increase in the scatter of individual points. It is worth noting that in these results, as in all those presented below, the viscous forces (ii) and (iii) defined in § 3 make a very small contribution. For case A, in which the ratio R_e/K_e had the lowest value, 7600, the magnitude of the resultant of forces (i), (ii) and (iii) exceeds that of the inertia force alone by about 1.3%; its phase lags that of the inertia force by about 0.7°. Taking the view that at a submergence $-y_0/c = 5$ interaction with the free surface is not a dominant factor in the flow around the cylinder (Chaplin, 1981), we conclude that the dependence of C_m on K_C is associated with nonlinear effects of viscosity, namely steady circulation and separation. Although no quantitative

Frequency / Case	0		ω		2ω	3ω
	C_{x04}	C_{y02}	$C_{x11} = C_{y11}$	$C_{x13} = C_{y13}$	$C_{x22} = C_{y22}$	$C_{x33} = C_{y33}$
B	0.019	0.13 (0.136)	1.90 (1.983)	−0.21	—	—
C	0.015	0.16 (0.155)	1.99 (2.061)	−0.36	0.081	—
D	—	0.25 (0.252)	1.96 (1.956)	−0.36	0.13	—
E	—	0.21 (0.214)	2.25 (2.246)	−0.58	0.44	0.15
F	—	0.32 (0.326)	2.03 (2.084)	−0.63	0.40	0.06
G	—	0.40 (0.444)	1.89 (1.867)	−1.30	0.37	0.32
H	—	0.64 (0.641)	1.81 (1.712)	—	0.52	—

TABLE 2. Dimensionless force coefficients for deep-water waves (figures in parentheses are derived from Ogilvie 1963)

agreement can be expected, the results are consistent with the concept on which (3.2) is based, to the extent that the observed nonlinear force opposes the inertia force, and is proportional to K_C^3. Furthermore, although the vertical and horizontal force components in waves of case A differ by about 8% (owing to the eccentricity of the orbital flow), there is no corresponding difference between the dimensionless results for the horizontal and vertical directions shown in figure 4 for $K_C < 2$. This has been achieved by plotting C_m derived from the vertical components of loading and acceleration against K_C derived from the horizontal velocity, and *vice versa*. This would be a natural way to plot the present data if it were known that the nonlinear force was proportional to the product of the uniform circulation and the perpendicular component of velocity.

From $K_C \approx 2$ there is a sudden increase in the loading, the results for the horizontal and vertical directions become distinct, and there is an increasing phase lag between the acceleration of the incident flow and the force. It is reasonable to attribute this behaviour to rapid growth of the wake and an increasing contribution from form drag acting in a direction which lags that of the acceleration. Also the observed scatter of the results in this region is a familiar characteristic of force measurements on cylinders in separated oscillatory flow.

Having investigated the flow and the loading for Keulegan–Carpenter numbers up to 3 for the deeply submerged case, the purpose of the remaining experiments was to determine the nonlinear forces in the lower K_C regime over a range of conditions in deep-water waves, including some cases with the cylinder close to the free surface. For each set of conditions, tests were carried out with a series of wave amplitudes limited either by clear evidence of separation in the force records of the type described above at $K_C = 2$, or by signs of instabilities in the incident waves. After each experiment, Fourier analysis of the data was carried out in order to isolate horizontal and vertical force components with frequencies 0, ω, 2ω and 3ω. From a series of results at each frequency for various wave amplitudes, contributions at orders up to the fourth in K_C were evaluated by least-squares analysis. Values of the resulting dimensionless coefficients defined by (2.1) are given in table 2. Some typical data (from cases B and E) are shown in figures 5–10.

For all conditions, $F_x^{(0)}$ was very much smaller than $F_y^{(0)}$, and only in cases B and C were the measurements of $F_x^{(0)}$ sufficiently free of noise to justify least-squares analysis. As shown in figure 5, it was then found to correlate well with K_C^4. The mean vertical force $F_y^{(0)}$ for case B is also shown in figure 5, and for K_C up to about 0.7 agrees well with the corresponding result from Ogilvie's theory. (All theoretical

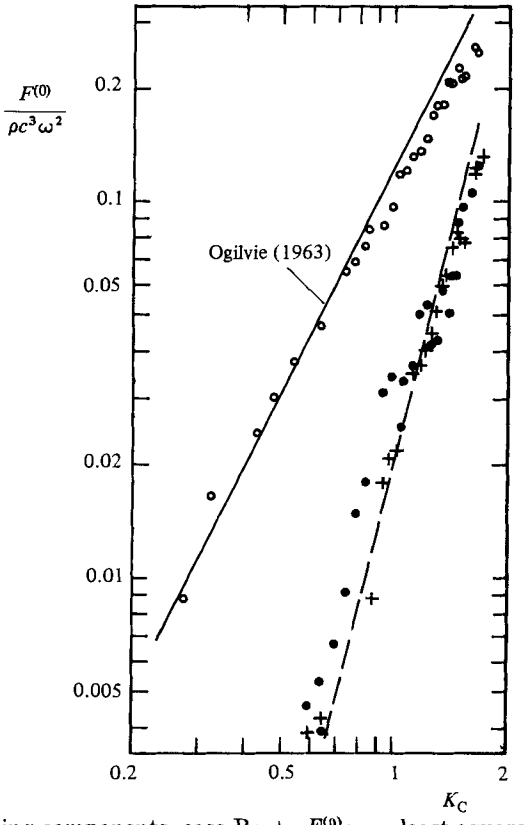

FIGURE 5. Steady-loading components, case B: +, $F_x^{(0)}$; ––, least-squares fit assuming that $F_x^{(0)}$ is proportional to K_C^4; ○, $F_y^{(0)}$; ●, departure of $F_y^{(0)}$ from linear theory.

results were computed using 20 terms in Ogilvie's expansion, and are indistinguishable from those derived from only 10.) For larger wave amplitudes there is a progressive departure from the theoretical result, suggesting an influence from higher-order terms. The differences between experimental and second-order theoretical results are also shown in figure 5, and suggest that there is a fourth-order contribution to $F_y^{(0)}$ of a magnitude similar to that of $F_x^{(0)}$. The inertia coefficient C_m derived from case B followed closely the behaviour of that from case A (figure 4), and yielded the same value, -0.21, for $C_{x13} = C_{y13}$.

Repeatable measurements of force at frequency 2ω were made in all experiments except B, and at frequency 3ω in cases E, F and G. Results for case E, in which the cylinder was much closer to the free surface, are shown in figures 6–10. With the cylinder at the highest elevation $y_0/c = -2$, its effect at the free surface was very clear. The waves were deformed as they passed, the largest ones breaking over the cylinder, and emerging with diminished amplitude and many frequency components. In these circumstances, the mean horizontal force (much smaller than either the fluctuating components or the mean vertical force) could not be resolved reliably from noise. However, the measured mean vertical force agrees well with the theoretical result as shown in figure 6; there is no evidence in this case of a higher-order contribution. Figure 7 shows the inertia coefficient C_m for case E; again the measurements depart gradually from the first-order result, and suggests that in these conditions form drag becomes significant from about $K_C = 1.5$.

Horizontal and vertical components of force at frequencies 2ω and 3ω are shown

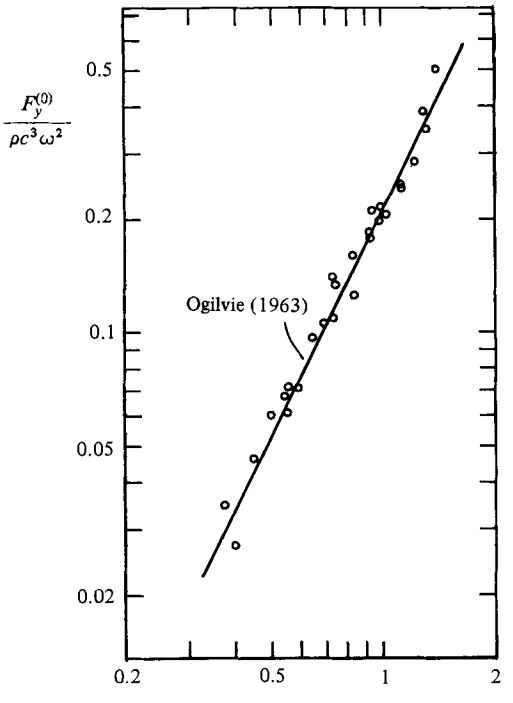

FIGURE 6

FIGURE 6. Steady vertical loading, case E.

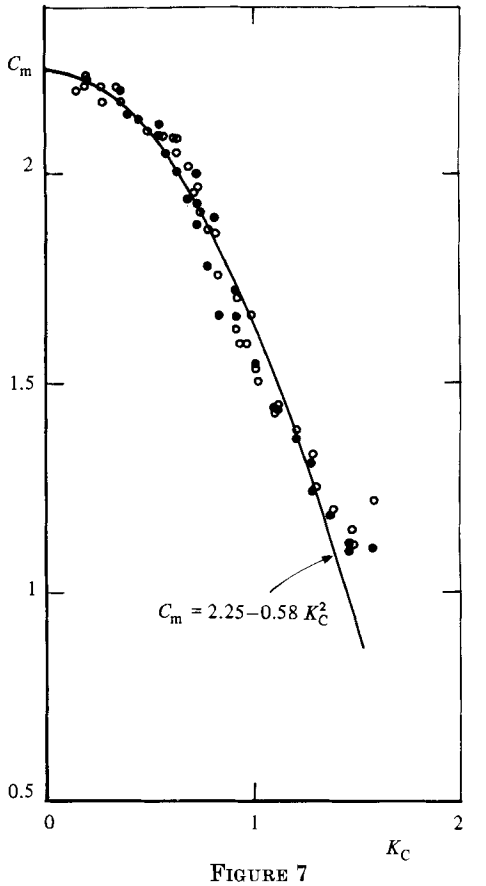

FIGURE 7

FIGURE 7. Inertia coefficient, case E: ●, horizontal force; ○, vertical force.

in figure 8. For K_C less than about 0.7 the two frequency components closely follow K_C^2 and K_C^3 respectively. Plotting the departure of the experimental results from these trends for larger waves revealed respectively third- and fourth-order components. Two-term polynomials were accordingly fitted to the data by least squares over the whole range of wave amplitudes, and are also shown in figure 8. The horizontal and vertical components of the forces at frequencies of both 2ω and 3ω were found to oscillate in quadrature, and indicated that the total force vectors at these frequencies are of steady magnitude and rotate uniformly, as is the case with the force at frequency ω. These relative phases are shown in figure 9, in which $\theta^{(2)}$ and $\theta^{(3)}$ denote the directions of the forces at frequencies 2ω and 3ω respectively, at the instant when the force at ω acts horizontally in the direction of wave advance.

Particularly for the larger wave amplitudes, the measured total forces were very much less than those derived by Ogilvie (1963). For a wave amplitude of 36 mm ($K_C = 1.47$) from case E, figure 10 compares the theoretical and experimental trajectories of the tip of the force vector; the large difference between the two results is predominantly due to the third-order component of force at frequency ω represented by $C_{x13} = C_{y13}$. In this example its effect is to reduce the inertia coeffieicnt for the cylinder from the theoretical value of 2.25 (greater than 2 owing to the proximity of the free surface) to 1.14. The influence of the higher-frequency components is also clear in the unequal spacing of the experimental points.

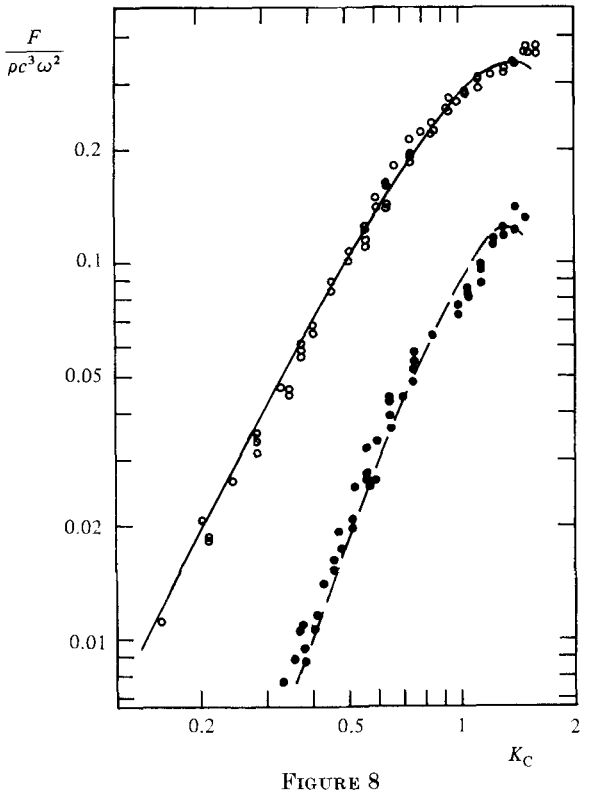

FIGURE 8

FIGURE 8. Loading components at frequencies 2ω and 3ω, case E: ○, $F_x^{(2)}$ and $F_y^{(2)}$; ——, least-squares polynomial with terms in K_C^2 and K_C^3; ●, $F_x^{(3)}$ and $F_y^{(3)}$; – –, least-squares polynomial with terms in K_C^3 and K_C^4.

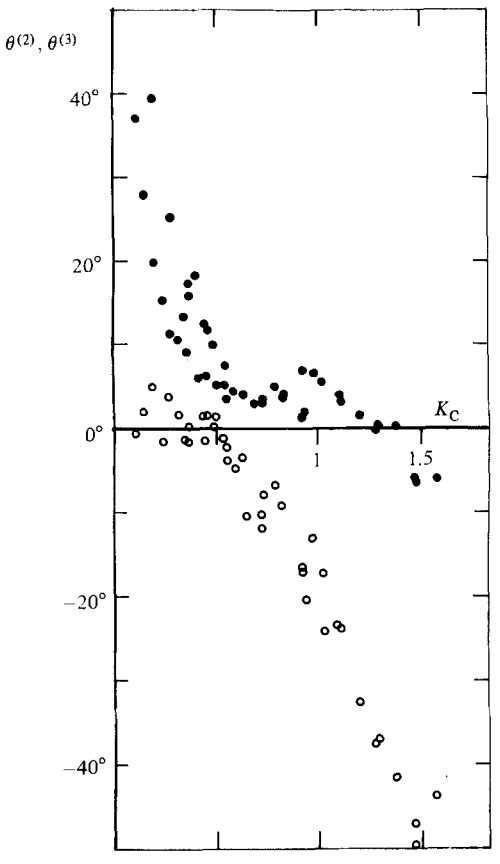

FIGURE 9

FIGURE 9. Phases of $F^{(2)}$ (●) and $F^{(3)}$ (○) with respect to $F^{(1)}$, case E.

The magnitudes of the measured linear and nonlinear forces expressed in dimensionless form in accordance with (2.1), set out in table 2, were derived by fitting to the data least-squares polynomials consisting of terms in K_C raised to those powers that were identified when the results were plotted on logarithmic axes as shown above. Ogilvie's results for $C_{x11} = C_{y11}$ and C_{y02} are in reasonable agreement with those derived from the measurements. Coefficients for the higher-order components of forces that were identified at frequencies 0, 2ω and 3ω are not presented, however, since their values are very sensitive to small systematic experimental errors. It is worth noting that for constant kc and kd the absolute value of $C_{x13} = C_{y13}$ increases as the submergence of the cylinder is reduced. It is reasonable to associate with this the increase in the inviscid-flow normalized tangential velocity around the cylinder (Chaplin 1981) and the effects of its increasing non-uniformity on the strength of the circulation (Riley 1971).

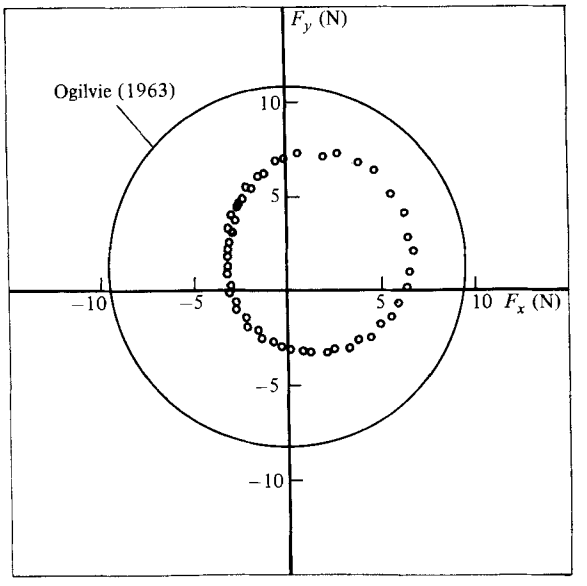

FIGURE 10. Force-vector plot for case E, with $a = 36$ mm, $K_C = 1.47$: ○, force measurements at intervals of 20 ms.

6. Reflected and transmitted waves

It is a conclusion from the classical first-order solution that from a submerged horizontal cylinder parallel with the crests there are no reflected waves. This is in agreement with the present experimental results to the extent that only in the conditions expected to give rise to the most severe inviscid-flow nonlinearities, namely the steepest waves of case H, could any reflection be detected. Reflection coefficients were obtained from the output of wave gauges situated at several different positions between the paddle and the cylinder by recording waves with and without the cylinder present, but in otherwise-identical conditions. Amplitudes and phases were almost identieal in both cases, except for the steepest waves of case H, in which the reflection coefficient increased to about 4% with the waves of the maximum amplitude 30 mm. Also in the region between the paddle and the cylinder there was no detectable change in the components of the profile of the waves at frequencies 2ω and 3ω.

On passing over the cylinder, the waves undergo a phase shift and acquire new frequency components. Phase shifts for the fundamental component calculated from the wave-gauge signals for case E are shown in figure 11, displaying trends that were clear also in the other cases where phase shifts were detected. For very small waves the results are in reasonable agreement with the linear theory (Ogilvie 1963), but for larger waves the phase lag is smaller than predicted, and in some cases for the steepest waves tested it became negative. This was observed in the analysis, not only of the sequence of 8 waves treated as a whole, but also of individual waves, some of which may have been influenced by reflections from the beach. However, the phase of the fundamental component of the force on the cylinder with respect to the phase of that of the incident waves differs very little from the theoretical result, over the range of wave amplitudes tested, as shown in figure 12.

Fourier analysis of wave records in the region between the cylinder and the beach revealed the higher-frequency components generated by interaction with the cylinder.

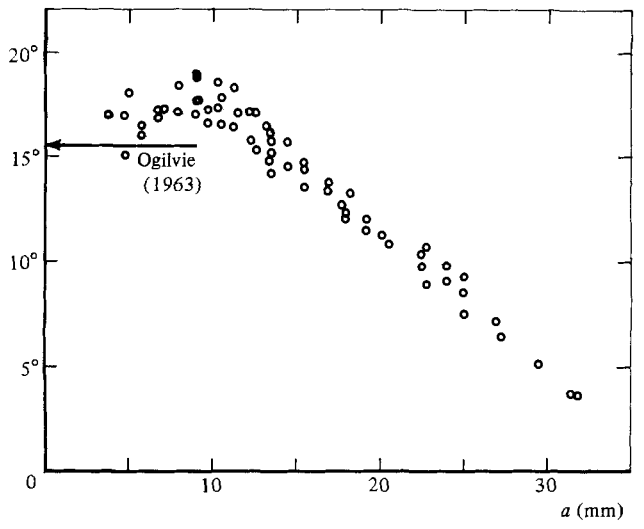

FIGURE 11. Wave phase lag at the fundamental wave frequency, case E.

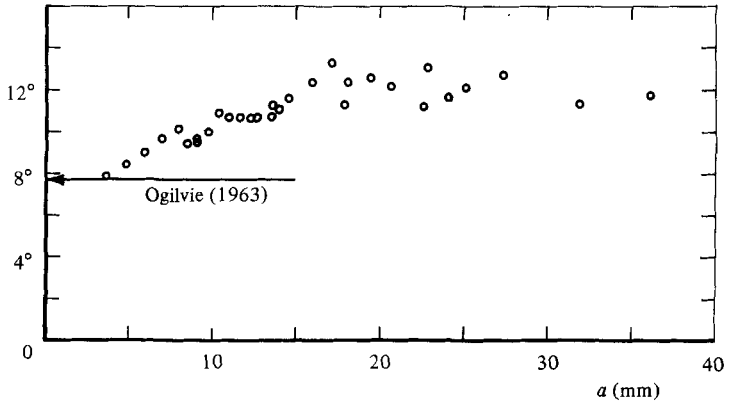

FIGURE 12. Force phase lag at the fundamental wave frequency, case E.

For the steeper waves tested the component at frequency 2ω of the free-surface elevation was as much as 20 % of that of the fundamental, or about 5 times the value corresponding to the 2ω-component of the incident waves.

7. Conclusions

The principal conclusion of this experimental work is that the oscillatory loading on a horizontal cylinder beneath waves may be as much as 50 % less than that predicted by linear theory, owing to a component of force shown to be proportional to the cube of the Keulegan–Carpenter number. For a deeply submerged cylinder in nearly circular orbital flow at Reynolds numbers of the order 10^4, it has been found that the inertia coefficient is given by

$$C_m = 2 - 0.21 K_C^2 \tag{7.1}$$

approximately, for $K_C < 2$. When the cylinder is closer to the free surface the nonlinear contribution to C_m is greater, but the value of K_C at which the force departs

from this relationship is reduced. Velocity measurements close to the cylinder suggest that the abrupt increase in loading for higher values of K_C is associated with the rapid development of the wake.

Other nonlinear contributions to the loading have also been identified in the present experiments. They include the time-independent part of the second-order vertical force, in reasonable agreement with the result derived by Ogilvie (1963) from the linear velocity potential, a time-independent fourth-order horizontal force, and fluctuating forces at frequencies respectively two and three times the fundamental wave frequency, at orders up to the fourth. These are, however, rather smaller than the nonlinear reduction to the inertia force.

Nonlinear forces are to be expected from the free-surface boundary condition and the effects of viscosity, but existing analyses of the flow do not reveal the relative importance of these factors. A numerical solution of the nonlinear inviscid-flow problem by Stansby & Slaouti (1984) produced results in agreement with the first-order fluctuating forces, suggesting that a strong nonlinear component, such as that apparent in (7.1), is not present in a potential-flow model. A feature of the viscous flow which may be responsible for nonlinear loading is the circulation generated around the cylinder by steady streaming.

Experimental measurements of the phase of the fluctuating force on the cylinder with respect to that of the incident waves were in reasonable agreement with linear theory over the whole range of wave amplitudes tested. However, the phase change that the waves undergo on passing over the cylinder was found with increasing wave amplitude to fall progressively below the theoretical value. In the ideal-fluid-flow calculations of Stansby & Slaouti (1984) the phase of the force remained close to the linear solution for all wave amplitudes, but phase changes in the waves were not calculated.

The author acknowledges support from the Marine Technology Directorate of the Science and Engineering Research Council. This project is part of the Fluid Loading programme of Marinetech North West, and was completed during a period of study leave granted to the author by the University of Liverpool. The cylinder used in the experiments was designed and initially tested by Andrew Miller.

REFERENCES

BATCHELOR, G. K. 1967 *An Introduction to Fluid Dynamics.* Cambridge University Press.

CHAPLIN, J. R. 1981 On the irrotational flow around a horizontal cylinder in waves. *Trans. ASME* E: *J. Appl. Mech.* **48**, 689–694.

CHAPLIN, J. R. 1984 Mass transport around a horizontal cylinder beneath waves. *J. Fluid Mech.* **140**, 175–187.

DEAN, W. R. 1948 On the reflexion of surface waves by a submerged circular cylinder. *Proc. Camb. Phil. Soc.* **44**, 483–491.

GRUE, J. & PALM, E. 1984 Reflection of surface waves by submerged cylinders. *Appl. Ocean Res.* **6**, 54–60.

LEPPINGTON, F. G. & SIEW, P. F. 1980 Scattering of surface waves by submerged cylinders. *Appl. Ocean Res.* **2**, 129–137.

LONGUET-HIGGINS, M. S. 1970 Steady currents induced by oscillations round islands. *J. Fluid Mech.* **42**, 701–720.

MEHLUM, E. 1980 A circular cylinder in water waves. *Appl. Ocean Res.* **2**, 171–177.

OGILVIE, T. F. 1963 First- and second-order forces on a cylinder submerged under a free surface. *J. Fluid Mech.* **16**, 451–472.

RILEY, N. 1971 Stirring of a viscous fluid. *Z. angew. Math. Phys.* **22**, 645–653.

RILEY, N. 1978 Circular oscillations of a cylinder in a viscous fluid. *Z. angew. Math. Phys.* **29**, 439–449.

STANSBY, P. K. & SLAOUTI, A. 1984 On non-linear wave interaction with cylindrical bodies: a vortex sheet approach. *Appl. Ocean Res.* **6**, 108–115.

URSELL, F. 1950 Surface waves in the presence of a submerged circular cylinder, I and II. *Proc. Camb. Phil. Soc.* **46**, 141–158.